

## A Simple Method to Synthesize Dy(OH)<sub>3</sub> and Dy<sub>2</sub>O<sub>3</sub> Nanotubes

An-Wu Xu,<sup>\*,†</sup> Yue-Ping Fang,<sup>†</sup> Li-Ping You,<sup>‡</sup> and Han-Qin Liu<sup>†</sup>

School of Chemistry and Chemical Engineering, Zhongshan University, Guangzhou 510275, China, and  
Electron Microscopy Laboratory, Peking University, Beijing 100084, China

Received November 1, 2002; E-mail: cedc17@zsu.edu.cn

Binary rare earth oxides are the most stable rare earth compounds, in which the rare earth ions hold typically a trivalent state.<sup>1</sup> Rare earth oxides have been widely used as high-performance luminescent devices, magnets, catalysts, and other functional materials based on the electronic, optical, and chemical characteristics arising from their 4f electrons.<sup>1</sup> Most of these advanced functions depend strongly on the compositions and structures, which are sensitive to the bonding states of rare earth atoms or ions. If rare earth oxides were fabricated in the form of a one-dimensional (1D) nanostructure, they would hold promise as highly functionalized materials as a result of both shape-specific and quantum confinement effects. They could also act as electrically, magnetically, or optically functional host materials.

Much attention has recently focused on 1D nanostructures with hollow interiors since the discovery of carbon nanotubes.<sup>2</sup> The unique physical and chemical properties of 1D nanotubes have been well documented and proposed for a wide range of applications.<sup>3</sup> The successful synthesis of nanotubes such as BN, WS<sub>2</sub>, MoS<sub>2</sub>, Bi, Te, NiCl<sub>2</sub>, VOx, and so forth has been reported.<sup>4</sup> Although several strategies have been developed for the growth of nanotubes, they suffer from the requirements of high temperature, special conditions, or tedious procedures. Catalyst- or template-based methods have been used to prepare nanotubes, such as carbon nanotubes, VOx, in which catalysts act as the energetically favored sites for the adsorption of gas-phase reactants, while the template is used to direct the growth of nanotubes.<sup>3b,4f</sup> However, the addition of a catalyst or a template to the reaction system involves a complicated process and may result in impurity in the products. One can overcome these difficulties by developing solution-phase methods for direct growth of the 1D nanostructure without involving catalysts or templates.<sup>5</sup> Recent studies on the preparation of semiconducting oxides nanobelts have shown that the 1D nanostructure can be prepared by evaporating the desired metal oxide powders at high temperatures,<sup>6</sup> which leads us to believe that the 1D nanostructure might be prepared via a dissolution–recrystallization process in the solution. Of the methods used in 1D nanostructure synthesis, hydrothermal processes have emerged as powerful tools for the fabrication of anisotropic nanomaterials.<sup>7</sup> However, no studies have been reported on the synthesis of Dy(OH)<sub>3</sub> and Dy<sub>2</sub>O<sub>3</sub> nanotubes to date. Here, we report a simple method for direct growth of the first Dy(OH)<sub>3</sub> nanotubes by facile hydrothermal treatment of bulk Dy<sub>2</sub>O<sub>3</sub> crystals.

In a typical synthesis, 0.8 g of Dy<sub>2</sub>O<sub>3</sub> powder (purity: 99.99%) was added to 20 mL of H<sub>2</sub>O and then poured into a stainless Teflon-lined 25-mL-capacity autoclave. The autoclave was maintained at 160 °C for 48 h and then air cooled to room temperature. The resulting products were collected and washed with water and dried at 60 °C in air. As-made Dy(OH)<sub>3</sub> was calcined to produce Dy<sub>2</sub>O<sub>3</sub> nanotubes in air at 450 °C for 6 h.

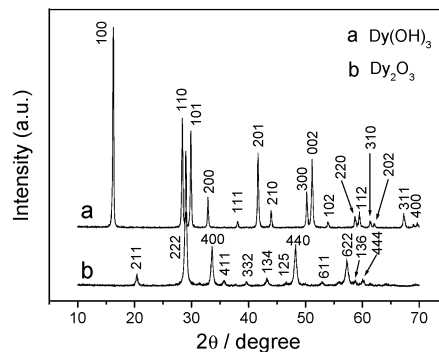


Figure 1. XRD pattern of the obtained Dy(OH)<sub>3</sub> and Dy<sub>2</sub>O<sub>3</sub> nanotubes.

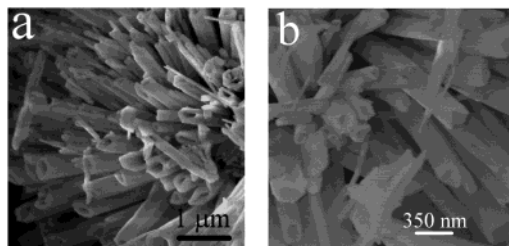


Figure 2. SEM images of the obtained Dy(OH)<sub>3</sub> (a) and Dy<sub>2</sub>O<sub>3</sub> (b) nanotubes.

The phase purity of the products was examined by X-ray diffraction (XRD) measurement performed on Rigaku X-ray diffractometer with Cu K $\alpha$  radiation. All of the peaks of the XRD pattern in Figure 1a can be readily indexed to a pure hexagonal phase [space group: *P6<sub>3</sub>/m* (176)] of Dy(OH)<sub>3</sub> with lattice constants *a* = 6.280 Å, *c* = 3.569 Å (JCPDS 19-0430). The XRD analysis indicates that the crystalline phase of the resulting products (Dy(OH)<sub>3</sub>) is different from that of the starting Dy<sub>2</sub>O<sub>3</sub> precursor (Supporting Information 1). Figure 1b shows that pure-phase Dy<sub>2</sub>O<sub>3</sub> can be obtained by calcination of as-made Dy(OH)<sub>3</sub>. All of the peaks can be indexed to a pure cubic phase [space group: *Ia $\bar{3}$*  (206)] of transformed Dy<sub>2</sub>O<sub>3</sub> with lattice constants *a* = 10.671 Å (JCPDS 86-1327). Thermogravimetric analysis indicates that Dy(OH)<sub>3</sub> has converted completely to Dy<sub>2</sub>O<sub>3</sub> at 450 °C by calcination (Supporting Information 2).

The morphology and structure of the products were examined with scanning electron microscopy (SEM, JEOL JSM-6330F). As shown in Figure 2a, the Dy(OH)<sub>3</sub> products consist almost entirely of nanotubes with outer diameters of 40–500 nm, inner diameters of 20–300 nm, and lengths ranging from 1 to 4 μm, in contrast to that of the starting material (Supporting Information 1). It can be seen that the tips of these tubes are open and have a hexagonal prism morphology. Dy<sub>2</sub>O<sub>3</sub> nanotubes was obtained from Dy(OH)<sub>3</sub> by calcination, which is clearly shown in Figure 2b. We find that Dy<sub>2</sub>O<sub>3</sub> tubes are smaller than Dy(OH)<sub>3</sub> tubes in that the density of

<sup>†</sup> Zhongshan University.

<sup>‡</sup> Peking University.

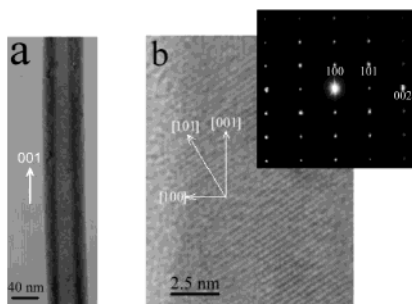


**Figure 3.** (a) TEM image of a single  $\text{Dy}(\text{OH})_3$  nanotube. (b) HRTEM image of the rim part of the tube wall with clearly resolved lattice fringe of (101) planes ( $d = 0.298$  nm). (Inset) SAED pattern recorded from the [010] zone axis.

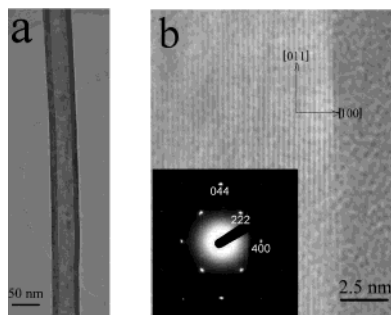


**Figure 4.** (a) TEM image of a single  $\text{Dy}_2\text{O}_3$  nanotube. (b) HRTEM image of the tube wall with clearly resolved lattice fringe of (400) planes ( $d = 0.267$  nm). (Inset) SAED pattern recorded from the [011] zone axis.

the former is higher than that of the latter. The results demonstrate that  $\text{Dy}(\text{OH})_3$  and  $\text{Dy}_2\text{O}_3$  nanotubes can be obtained by this simple method.

The tubular structure of the products were further examined with transmission electron microscopy (TEM) and high-resolution TEM (JEOL-2010 at 200 kV). Figure 3a shows the low magnification TEM image of a typical  $\text{Dy}(\text{OH})_3$  tube with the diameter ca. 60 nm. Figure 3b is the HRTEM image with the clearly resolved interplanar distance  $d_{101} = 0.298$  nm; the nanotubes grow along the [001] direction (the  $c$  axis). The selected area electron diffraction (SAED) pattern (inset in Figure 3b) taken from this nanotube can be indexed as a hexagonal  $\text{Dy}(\text{OH})_3$  single crystal recorded from the [010] zone axis. TEM observations show that each tube is a single crystal. TEM image of the embedded sample (Supporting Information 3) shows the cross sections of nanotubes, confirming that the tubes are really empty. Figure 4a shows a single  $\text{Dy}_2\text{O}_3$  nanotube. The SAED (inset in Figure 4b) pattern taken from a single nanotube can be indexed as a cubic  $\text{Dy}_2\text{O}_3$  single crystal recorded from the [011] zone axis. Figure 4b is the corresponding HRTEM image with the clearly resolved interplanar distance  $d_{400} = 0.267$  nm. The (400) planes are oriented parallel to the nanotube growth axis. The synthesis of  $\text{Dy}(\text{OH})_3$  and  $\text{Dy}_2\text{O}_3$  nanotubes can easily be reproduced and scaled up. Using a large autoclave (800 mL) for the hydrothermal treatment, several tens of grams of the nanotubes can be obtained.

We also prepared  $\text{Ho}(\text{OH})_3$  nanotubes starting from bulky  $\text{Ho}_2\text{O}_3$  crystals by the same method. The tubular structure of  $\text{Ho}(\text{OH})_3$  is

clearly shown in the Supporting Information 4.  $\text{Ho}(\text{OH})_3$  nanotubes was calcined to produce  $\text{Ho}_2\text{O}_3$  nanotubes. Although the exact mechanism for the formation of these tubular nanostructures is still unclear, we believe that the growth of the nanotubes is not catalyst-assisted or template-directed. Because the only source material used in our synthesis is pure rare earth oxide crystals, it is likely that the growth is governed by a solution-solid process (SS), in which the oxide molecules dissolved and hydroxylated from the starting oxide under hydrothermal treatment, subsequently to recrystallize and grow into tubular nanostructures through a dissolution–recrystallization process.<sup>8</sup> It is obvious that bulk particles are the precursors for further crystal growth rather than ionic species, an important difference to previous reports based on a homogeneous nucleation and solution growth process.<sup>5b,9</sup> We propose a related SS mechanism in which the precursor is delivered in a solution rather than in the vapor phase, an analogy to the vapor-solid (VS) process for nanobelts growth.<sup>6,10</sup>

In summary, we have found a simple route to prepare single-crystal  $\text{Dy}(\text{OH})_3$  and  $\text{Dy}_2\text{O}_3$  nanotubes by facile hydrothermal treatment. Such nanotubes with open ends have a variety of promising applications. The simplicity of hydrothermal process, cheapness, and availability of raw materials are advantages favoring the scaling-up of nanotubes. Rare-earth oxide nanotubes could be doped with different rare-earth elements and used for fabricating nanosize optical devices based on the characteristics of individual nanotubes. Further work is under way to study the formation mechanism and properties of this novel tubular morphology, and the possibility of synthesizing other nanotubes.

**Acknowledgment.** This work was supported by the Guangdong Province Key Project (20010185C).

**Supporting Information Available:** XRD and thermogravimetric analyses and TEM and SEM images (PDF). This material is available free of charge via the Internet at <http://pubs.acs.org>.

## References

- (1) (a) Adachi, G. Y.; Imanaka, N. *Chem. Rev.* **1998**, *98*, 1479. (b) Xu, A. W.; Gao, Y.; Liu, H. Q. *J. Catal.* **2002**, *207*, 151.
- (2) Iijima, S. *Nature* **1991**, *354*, 56.
- (3) (a) Ajayan, P. M. *Chem. Rev.* **1999**, *99*, 1787. (b) Rao, C. N. R.; Satishkumar, B. C.; Govindaraj, A.; Nath, M. *ChemPhysChem* **2001**, *2*, 78.
- (4) (a) Chopra, N. G.; Luyren, R. J.; Cherry, K.; Crespi, V. H.; Cohen, M. L.; Louis, S. G.; Zettle, A. *Science* **1995**, *269*, 966. (b) Tenne, R.; Margulis, L.; Genut, M.; Hodes, G. *Nature* **1992**, *360*, 444. (c) Feldman, Y.; Wasserman, E.; Srolovita, D. J.; Tenne, R. *Science* **1995**, *267*, 222. (d) Li, Y. D.; Wang, J. W.; Deng, Z. X.; Wu, Y. Y.; Sun, X. M.; Yu, D. P.; Yang, P. D. *J. Am. Chem. Soc.* **2001**, *123*, 9904. (e) Hachohen, Y. R.; Grunbaum, E.; Sloan, J.; Hutchison, J. L.; Tenne, R. *Nature* **1998**, *395*, 336. (f) Niederberger, M.; Muhr, H.-J.; Krumeich, F.; Bieri, F.; Günther, D.; Nesper, R. *Chem. Mater.* **2000**, *12*, 1995. (g) Yada, M.; Mihara, M.; Mouri, S.; Kuroki, M.; Kijima, T. *Adv. Mater.* **2002**, *14*, 309.
- (5) (a) Kasuga, T.; Hiramatsu, M.; Hoson, A.; Sekino, T.; Niihara, K. *Adv. Mater.* **1999**, *11*, 1307. (b) Wang, X.; Li, Y. D. *J. Am. Chem. Soc.* **2002**, *124*, 2880.
- (6) Pan, Z. W.; Dai, Z. R.; Wang, Z. L. *Science* **2001**, *291*, 1947.
- (7) Patzke, G. R.; Krumeich, F.; Nesper, R. *Angew. Chem., Int. Ed.* **2002**, *41*, 2446.
- (8) Lu, J.; Xie, Y.; Xu, F.; Zhu, L. Y. *J. Mater. Chem.* **2002**, *12*, 2755.
- (9) Mayers, B.; Xia, Y. N. *Adv. Mater.* **2002**, *14*, 279.
- (10) (a) Brenner, S. S.; Sears, G. W. *Acta Metall. Mater.* **1956**, *4*, 268. (b) Yang, P.; Lieber, C. M. *J. Mater. Res.* **1997**, *12*, 2981.

JA029181Q